Growth of alkali halides by molecular-beam epitaxy

M. H. Yang and C. P. Flynn
Department of Physics, University of Illinois at Urbana-Champaign, 1110 West Green Street, Urbana, Illinois 61801 and Materials Research Laboratory, University of Illinois at Urbana-Champaign, 104 South Goodwin Avenue, Urbana, Illinois 61801
(Received 11 December 1989)

Alkali halide single crystals are shown to grow well from molecular beams over a wide temperature range $\sim(0.1-0.5)T_m$, where T_m is the melting temperature. Growth characteristics for homoepitaxy and heteroepitaxy, for alloys and superlattices, are discussed and found systematically different from those of metals and semiconductors. The reasons are related here to the type of lattice cohesion.

I. INTRODUCTION

There is a lack of research in which crystal growth by molecular-beam epitaxy (MBE) has been investigated for strongly ionic materials. This stands in marked contrast to the very large and rapidly swelling literature on the MBE growth of semiconductors,[1,2] and the considerable recent effort in metals MBE.[1,3-5] Both these latter fields are driven, in part, by technical opportunities.[1-3] While most semiconductor studies have concerned group-IV elemental (i.e. Si, Ge) materials or III-IV compounds,[1,2] a substantial effort has also been devoted to II-VI compounds,[1] which are partially ionic. An understanding of universal growth behavior in the form of scaling of equivalent states was achieved for the first time for metal with the explanation[5] why metal interfaces can be grown smooth and sharp by MBE only at a growth temperature $T_g \sim 3T_m/8$, with T_m the absolute melting temperature. Similar scaling of growth temperature for elemental semiconductors, characteristically different from the case of metals, has since been pointed out.[6] Strongly ionic solids are a third, distinct type of material, with their own characteristic bonding behavior, which could reasonably be expected to influence the growth behavior. The present research was undertaken with the aim of exploring the growth characteristics of strongly ionic solids in order to further a global understanding of the way MBE growth behavior changes from one material type to the next.

Alkali halide crystals with the rocksalt structure play the role of model ionic materials. Theory and experiment agree that almost a full unit charge is transferred from cation to anion sites.[7] Even including ionic distortions, for example, the effective ionic charge found from a comparison of longitudinal and transverse optical phonon frequencies approaches $0.9e$.[8] Bulk thermodynamic properties of these model compounds have been widely studied, including many pseudobinary phase diagrams,[9] which show they are generally miscible if the misfits are about 5% or less and not miscible if the misfits are about 10% or larger. There is little or no tendency to form ternary- or quaternary-ordered compounds in the bulk. Diffusion and conductivity in alkali halides have been examined in many case and a good basis exists for understanding atomic mobility in the bulk.[10] Vacancy diffusion is dominant. The diffusion coefficients on the anion and cation sublattices are similar to those of metals near the melting temperatures ($\sim 10^{-8}$ cm^2/sec).[10] Anions and cations generally have similar activation energies. These roughly scale with the melting temperature, so that bulk diffusion in simple salts is quite similar to the well-known behavior in metals,[5] where the bulk diffusion scales with corresponding states remarkably accurately.

The properties of alkali halide surfaces are much less well understood, although a basic theoretical framework has been in place for three decades. Only low-energy surfaces are of experimental interest and of these (100) planes of easy cleavage are the most important. The (100) terraces have square symmetry and are electrically neutral, as may be verified in Fig. 1. A number of researchers[11-13] have studied adsorption and desorption of molecules at the (100) terraces of cleaved alkali halide (100) surfaces at high temperature and the corresponding interaction between the vapor phase and the (100) surface. Of particular interest are energetics of molecular binding to ledges[12] and nucleation of new holes in nearly perfect (100) terraces, with or without the promoting effects of impurities.[11,13] A semi-empirical calculation for several alkali halides by Bjorund and Spears[12] showed these diatomic molecules prefer to maintain their molecular interatomic separation on the (100) terraces, while calculations by Hove,[14] who has adapted the Born model of alkali halide cohesion, explain why the ionic molecule and the separate ions all bond quite weakly to (100) terraces. By far the largest energy in the problem is the binding energy of the ionic molecules, typically about 5 eV. The cohesion of the solid is further 1-2 eV. This is mainly released when the ionic molecule is attached in the correct orientation to a surface ledge joining two terraces differing in height by one atomic step, as shown in Fig. 1. The bonding of the ionic molecule (or of the separate anion or cation) to the (100) terraces is quite weak, typically ~ 0.3 eV. There is good reason why this should be a general characteristic of strongly ionic solids. A solution of Laplace's equation with wave vector q in the xy plane must fall off with z as $\exp(iq_x x - |q_z|z)$, for

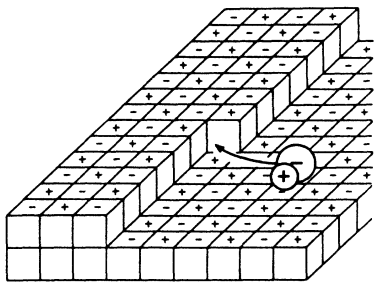

FIG. 1. Sketch of rocksalt (100) terraces, with a ledge to which molecular species bond strongly.

example. This exponential weakening of the corrugated surface field leads to generally weak surface adhesion and, correspondingly, to extremely high mobility of surface species on the terraces, with activation energies ~ 0.2 eV. The energetics are summarized in Fig. 2.

The present work was undertaken in an effort to control and understand the growth behavior of ionic materials. It is part of a broad program that explores strongly ionic oxides also. In the light of the energetic factors described above it appears reasonable to initiate studies of alkali halide grown by deposition of ionic molecule on (100) cleaved terraces. Some observations involving (111) terraces will also be mentioned. The work described below reveals that MBE growth of alkali halides is dominated by the characteristically weak terrace interaction and strong ledge interaction offered by the (100) surfaces. In other research to be reported elsewhere we have found similar results for MgO, a strongly ionic oxide, so that there appears to be reason to believe that the behavior is part of a much broader pattern. Only the alkali halide results are reported here. In Sec. II the MBE equipment is discussed, and Sec. III presents the experimental results. Section IV places the results in the context of theoretical ideas described above. A preliminary account of the work has been published elsewhere.[15]

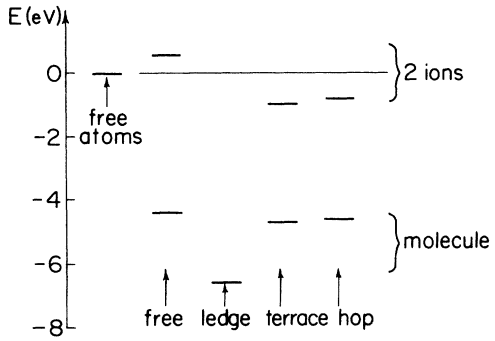

FIG. 2. Energetics of separated K^+ and Cl^-ion (top) and KCl molecules (bottom), free (column 2), in the crystal (i.e., on ledge, column 3), on a terrace (column 4), and the activation energy during surface migration (column 5). Column 1 shows the energy zero as neutral K and Cl atoms. Columns 4 and 5 for ions differ by the calculated K^+ activation energy of 0.23 eV (Ref. 17).

II. EXPERIMENTAL METHOD

Crystal growth took place in a homemade MBE chamber equipped with four effusion cell sources, two 6-MHz quartz crystals and a quadrupole mass spectrometer. The growth configuration was vertical and the sample holder was introduced from the top of the chamber while the alkali halide effusion cells were positioned at the bottom facing upwards. The quartz crystals and the quadrupole mass spectrometer were held close to the sample holder. Substrates were fastened to the sample holder block, made of tantalum or copper, by indium solder which also served to provide the thermal contact between the substrate and sample holder. The nominal substrate temperature could be varied from 1200 to 120 K by resistive heating and liquid-nitrogen cooling. Each effusion cell had its own shutter and the alkali halide charge was isolated from the PBN (pyrolytic boron nitride) crucible by a tantalum tube to avoid any reaction between the two. The tantalum tube was fixed to a stainless-steel sleeve which extended into the MBE chamber to define the spread of the reactive alkali halide species involved. This attachment proved thermally sluggish but provided good stability over extended periods, once equilibrated.

Substrates were prepared by cleaving selected alkali halide single crystals in air on a (100) plane typically 1 cm $\times$ 1cm in size. The cleaved alkali halide face normally preserved a high-quality surface. It was suitable for the MBE growth of alkali halide crystals after overnight heating under vacuum at 250 °C or higher. Much higher temperatures ~ 600 °C were needed for LiF crystals. In all cases, when heated to $0.65T_m$, the alkali halide crystal surface evaporated at a significant rate, which resulted in visible improvements of surface quality. Additional improvement to the surface could be accomplished by homoepitaxial regrowth at moderate rate ~ 1 Å/sec, which further smooths the surface. As an example Fig. 3(a) shows the reflection-high-energy electron diffraction (RHEED) patterns of the air-cleaved (100) NaCl surface after the above treatment. Care was required with RHEED observation of alkali halides because the electron beam damages their surfaces, which desorb, most

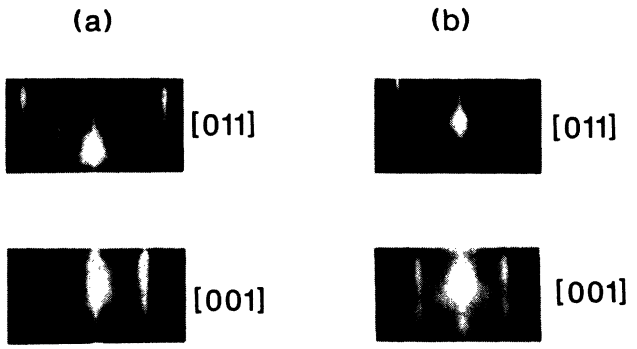

FIG. 3. RHEED patterns of (a) cleaved and evaporated NaCl after 200-Å regrowth at room temperature and (b) KBr(100) after 2 μm regrowth at -145 °C. See text for details.

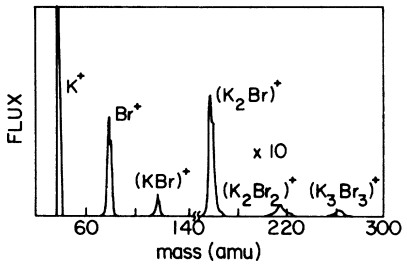

FIG. 4. A typical mass spectrum of KBr vapor during growth.

probably by Auger related mechanisms.[16] In our experiments the electron beam was only allowed to focus on the sample surface for the short period of time required to photograph the RHEED pattern, and the beam was then removed. The ability to evaporate an epitaxial structure away after study is an obvious convenience, permitting multiple uses of each substrate.

Deposition depths were determined by means of two independent quartz crystals capable of monitoring controlled deposition rates ranging from 0.1 to 100 Å/sec. The two quartz crystals made it possible to determine the deposition rate and the total deposition at any time during the growth of pseudobinary alloys and superlattices. Trimers, dimers, and monomers of alkali halide molecules were observed by means of the quadrupole mass spectrometer. An example of a typical mass spectrum from a KBr molecular beam is shown in Fig. 4. The molecules are generally fragmented by the ionizer of a mass spectrometer.[17] Therefore, the dominant M^+X^- monomer in the molecular beam, where M^+ and X^- are alkali and halide ions, respectively, was observed mainly as an increase of M and X above their high background levels. This made quartz-crystal measurement essential since the background produced no deposition on either the substrate or the quartz crystal. A calibration of the quartz crystal was obtained by growing a thick alkali halide film with (111) orientation on a macroscopically smooth (0001) sapphire substrate (α Al_2O_3) and the film thickness determined directly after growth by α step measurements of the deep steps caused by wires masking the deposition. It was difficult to use this method directly for alkali halides grown on cleaved (100) surfaces because cleavage leaves many steps comparable to or larger in thickness than the grown film.

III. EXPERIMENTAL RESULTS

A. Homoepitaxial growth

Smooth epitaxial regrowth from the molecular beam took place readily in most cases for a range of temperatures below $0.5T_m$. An example given above in Sec. II is the regrowth of 200 Å of NaCl at room temperature [see Fig. 3(a)]. It is of considerable interest to note, as we document below, that this high-quality epitaxial regrowth persists even at rates >10 Å/sec and at temperatures down to -150 °C at which the substrate cooling reached its limit. We have established that this nominal growth

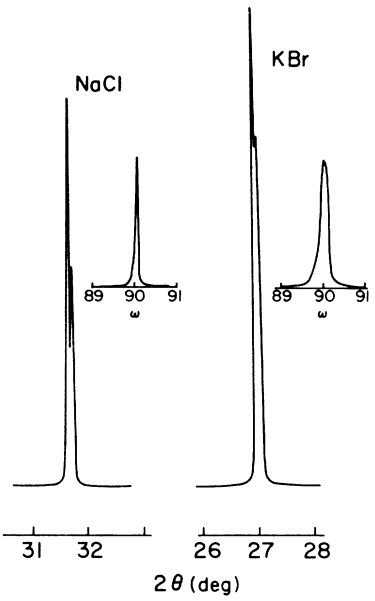

FIG. 5. X-ray Bragg scans and their rocking curves (insets) of NaCl substrate and thick KBr epilayer, showing coherence length $\sim 10^3$ Å and mosaic spread $\sim 0.3°$.

temperature T_g was not in serious error owing to radiation heat from the effusion cell source. The substrate was indium soldered to a massive copper block. Neither added shielding of the effusion cell source nor the periodic opening and closing of the shutter made any significant change in the RHEED pattern.

Figure 3(b) shows the RHEED spectra of a KBr(100) film for [001] and [011] azimuths taken after ~ 2 μm regrowth at -145 °C in a growth process described below. NaCl(100) was used as the substrate; its surface exhibited RHEED patterns similar to those in Fig. 3(a). The NaCl substrate was treated as described in Sec. II, and 300 Å of KBr grown at 0 °C. The first 10 Å of the deposition was at a rate 0.2 Å/sec, followed by 0.6 Å/sec for the next 140 Å and 1 Å/sec for the last 150 Å. Further comments on heteroepitaxial aspects are presented below. Here we discuss the homoepitaxial growth of KBr on the substrate so prepared. With a constant growth rate at about 1 Å/sec the substrate temperature was gradually lowered to -145 °C over the course of about 2 h. Once the substrate temperature reached its lowest limit, the growth rate was gradually increased from 1 Å/sec to nearly 100 Å/sec. The RHEED patterns remained the same as those shown in Fig. 3(b) throughout the growth.

X rays were used to evaluate the bulk quality of the MBE grown crystals. As an example, Fig. 5 compares the (200) x-ray Bragg scan and rocking curve of the KBr epilayer described above with those of the substrate NaCl crystal on which the KBr was grown. Note that most of the 2-μm thick KBr film was grown at rate above 50 Å/sec on a substrate whose temperature was held near -150 °C. As shown in the figure, the Cu $K_{\alpha 1}$-$K_{\alpha 2}$ splitting clearly observed in the substrate NaCl Bragg scan also remains partly visible for the KBr epilayer. The mosaic spread of $\sim 0.3°$ is only 0.2° larger than that of the substrate. The structural coherence length of the KBr

epilayer was estimated to be $\sim 10^3$ Å.[18]

Crystals of NaCl, NaI, KCl, KI, RbCl, RbI, and LiF were grown under similar conditions to those described above for KBr. All proved consistent with a universal growth characteristic that regrowth on alkali halide (100) surfaces can take place rapidly at growth temperature T_g as low as $0.11T_m$. It is possible that smooth growth continues down to still lower temperatures. Unfortunately we could not continue the investigation to lower T_g owing to the limitation on the substrate cooling system. We show later that this corresponds to surface mobility with a typical activation energy $E_s \sim 0.2$ eV for ionic molecules on the (100) terraces of alkali halide crystals.

B. Heteroepitaxy

Alkali halide crystals span a wide range of lattice constants. Therefore, heteroepitaxial growth generally takes place between substrate and epilayer crystals with large misfits. When a second alkali halide is grown on a foreign alkali halide surface, the pseudomorphically strained state persists for a thickness which depends on the lattice misfit. Once the epilayer film relaxes to its own lattice spacing, its surface as verified by *in situ* RHEED observation becomes progressively better as the growth continues. An exception occurred for fluorides on nonfluorides for which nucleation problems evidently prevented smooth growth from the very beginning.

Figure 6(a) compares RHEED spectra from two different thicknesses of KCl crystals grown on RbCl(100) with that of the RbCl substrate. KCL and RbCl crystals have a lattice mismatch of 4.7%, the smallest in this study. The substrate temperature was 200 °C and the deposition rate was held at 1 Å/sec. It is quite evident that the pseudomorphically strained KCl crystal grew very well. When the thickness approaches 32 Å the KCl relaxed to its own bulk lattice spacing and the RHEED spectrum deteriorated somewhat. After 500 Å of growth, the RHEED spectrum became as good as that of the original RbCl substrate.

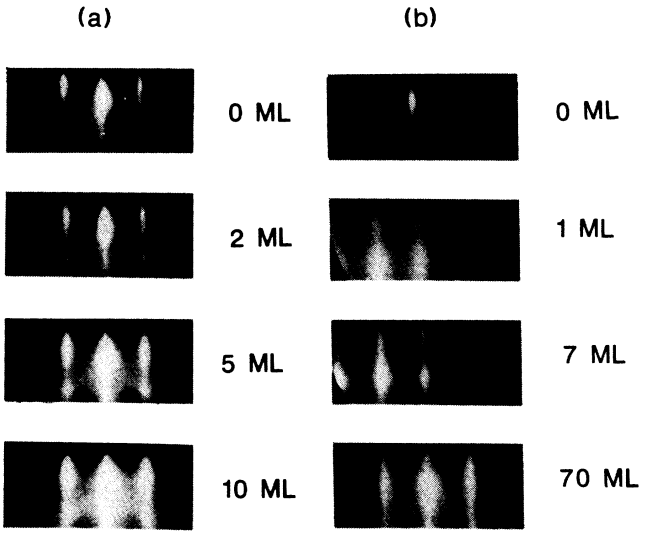

FIG. 7. RHEED patterns of NaCl with different thicknesses grown on KCl at (a) 200 °C and (b) −60 °C.

For larger lattice misfits the thickness of the stable pseudomorphically strained state decreases. Figure 7(a) shows results for heteroepitaxial growth of ten monolayers of NaCl on KCl(100), where the lattice mismatch is $\sim 10.5\%$. The growth took place at 200 °C with a deposition rate of 0.02 Å/sec for the first 140 Å and 0.07 Å/sec for the last 160 Å. Slow growth rates were chosen so that the amount of deposition could be controlled to within one monolayer. As shown in Fig. 7(a), the strained NaCl film with the in-plane lattice spacing of KCl persisted for about five monolayers, at which point the RHEED spectrum shows some indication of the streaks splitting. These became very clear after ten monolayers of NaCl. The new wider streaks correspond to diffraction from NaCl whose lattice parameter is al-

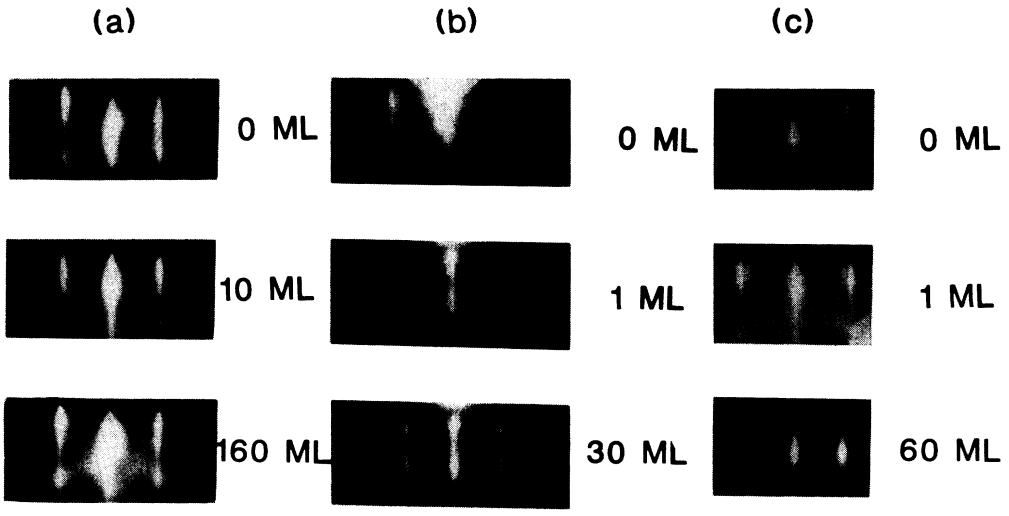

FIG. 6. Comparison of RHEED patterns of (a) KCl with different thicknesses grown on a RbCl substrate, (b) KBr grown on NaCl at 0 °C, and (c) RbCl grown on NaCl at 200 °C.

most the same as that of the bulk NaCl. Evidently the NaCl overlayer partially relaxes to its own lattice spacing at this thickness. When the KCl substrate was cooled to a lower temperature, $T_g = -60\,^{\circ}\mathrm{C}$, the heteroepitaxial growth of NaCl took place somewhat differently. As shown in Fig. 7(b), the first few monolayers of NaCl showed a poor diffraction pattern with diffuse streaks and strong background scattering. The wider spacing of the NaCl visible between the RHEED streaks indicates the relaxation occurred during the first monolayer of growth. As the thickness of NaCl increased, the quality of the RHEED spectrum improved significantly.

When the lattice misfit between the two alkali halides becomes as large as $\sim 15\%$, the overlayer generally appears to relax within the first monolayer. Figures 6(b) and 6(c) shown *in situ* RHEED spectra for KBr grown on NaCl and RbCl grown on NaCl, respectively. The lattice misfits of the KBr/NaCl and RbCl/NaCl systems are 14.6% and 15.2%, respectively. In both cases RHEED spectra indicate that relaxation took place within the first monolayer. For KBr/NaCl grown at 0 °C, RHEED showed diffuse diffraction streaks with strong background scattering while for the RbCl/NaCl grown at the higher temperature of $T_g = 200\,^{\circ}\mathrm{C}$, the RHEED spectra showed much sharper double streaks with less background scattering. As observed above, the quality of the overlayer film showed significant improvement after 500 Å of regrowth, both for KBr and RbCl.

Unlike the rest of alkali halide family, alkali fluorides generally grew poorly on foreign alkali halide substrates, even after several hundred Angstroms of growth. This may possibly be due to their higher molecular binding energy. As an example, Figs. 8(a) and 8(b) show the RHEED spectra of KF grown on NaCl(100) and KCl(100), respectively. For KF/NaCl, where the lattice mismatch is about 5%, we observed at $T_g = 250\,^{\circ}\mathrm{C}$ that the KF film grew as a single crystal for about 500 Å. During this growth it was possible to observe a gradually deteriorating RHEED pattern. Only the background scattering remained after 500 Å. At about 10-Å thickness the KF film was highly distorted, as indicated by three times the expected number of diffraction spots. As growth continued the film gradually relaxed its structure. Throughout this growth, the surface of the film was quite rough, as indicated by lack of streaks in the RHEED spectra, and it slowly deteriorated as the film thickness increased. For KF/KCl where the lattice mismatch is $\sim 12\%$, which is significantly larger than that of KF/NaCl, the KF film as grown was found to be relaxed within the first monolayer. The RHEED pattern shown in Fig. 8(b) displays broad diffuse streaks which did not improve as the film thickness increased in the way observed in nonfluorides. Similar results were obtained in the heteroepitaxial growth of NaF and RbF.

The growth of KBr, KBCl, and RbCl on single crystals of commercially available epitaxial-grade sapphire (α-Al_2O_3) was also studied. All three salts exhibit the same growth characteristics. As an example, Fig. 8(c) displays RHEED spectra of KBr grown on the (0001) surface of a sapphire single crystal. The normal direction of the KBr film grown on this sapphire surface was identified as the (111) orientation. Because the cube faces are the lowest in energy for fcc alkali halide crystals, the observed three-dimensional (3D) growth of alkali halide with (111) orientation is not surprising. In fact, the RHEED patterns suggest that each island facets to form the three cubic faces. The 3D growth remains rapid at $T_g \sim -150\,^{\circ}\mathrm{C}$ just as in the case where the growth took place on alkali halides (100) surface.

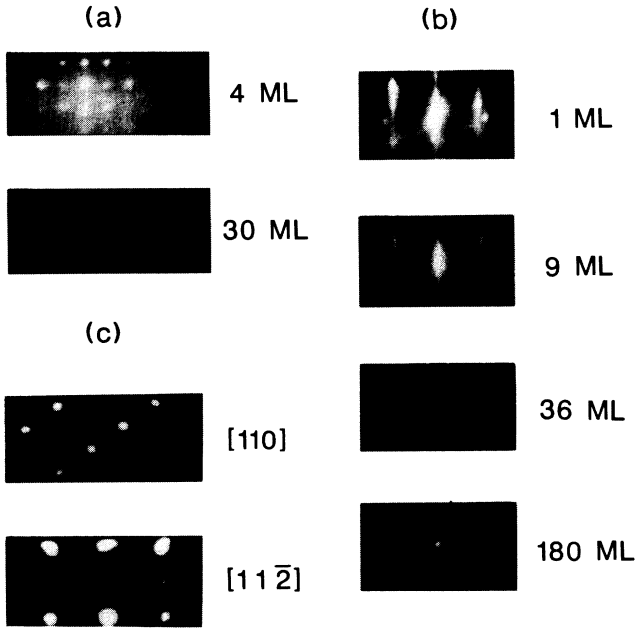

FIG. 8. RHEED patterns of (a) KF grown on NaCl, (b) KF grown on KCl, (c) KBr (111) grown on α-Al_2O_3(0001).

C. Metastable pseudobinary alloys

We have observed by x-ray diffraction, and for some systems by in situ RHEED also, that when two immiscible alkali halides are deposited simultaneously on a suitable lattice-matched substrate they usually segregate into oriented columnar growths of the almost pure salts. An example of such growth is RbF-RbI grown on the (100) surface of RbCl, whose lattice constant is almost equal to the average for RbF and RbI. Results of an x-ray diffraction study of this system grown at 100 °C are shown in Fig. 9(a). The segregated RbI clusters had

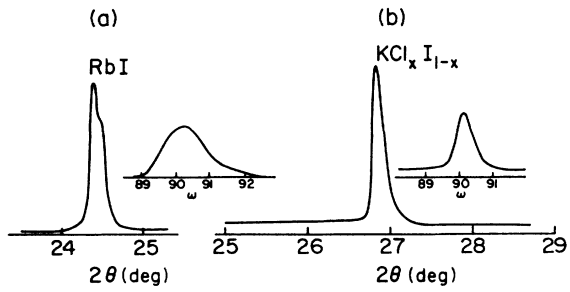

FIG. 9. X-ray Bragg scan and rocking curve (inset) of (a) the segregated pure salt RbI in a $RbF_{0.5}I_{0.5}$ "alloy" grown on RbCl, (b) KCl_xI_{1-x} alloy with $x \sim 0.5$ grown on KBr.

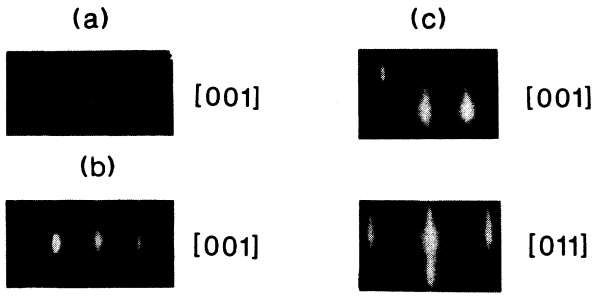

FIG. 10. RHEED patterns of (a) $RbF_{0.5}I_{0.5}$ approximately ten monolayers thick grown on RbCl, (b) KCl_xI_{1-x} with $x \sim 0.5$ grown on KBr, and (c) (KCl/RbCl) superlattice with 50 periods and a wavelength of ~ 50 Å, grown at -50°C. The segregation of $RbF_{0.5}I_{0.5}$ into pure salts of RbF and RbI are shown clearly by the two sets of streaks in (a).

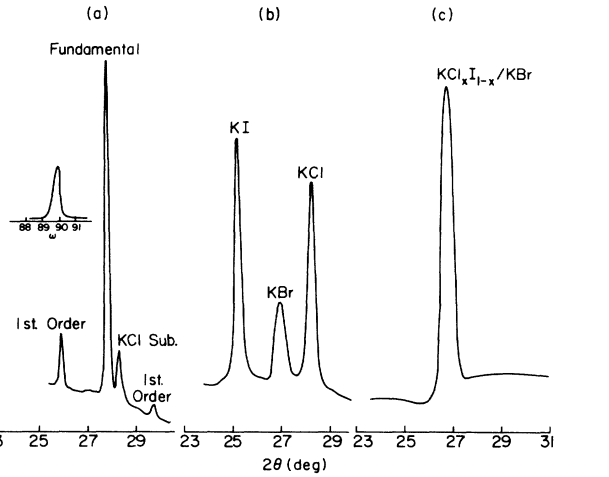

FIG. 11. (a) Bragg scan of a (KCl/RbCl) superlattice with 50 periods and a wavelength of ~ 50 Å, grown at -50°C. First-order satellites are visible at either side of fundamental reflection about 2° away. The inset shows the rocking curve of the fundamental reflection. (b) Bragg scan of a sample grown by alternating depositon of KCl and of KI monolayers. The broad diffraction peak near 27° suggests that a poor quality $KCl_{0.5}I_{0.5}$ alloy was formed. (c) Bragg scan of a sample grown by alternating deposition five monolayers of KCl and KI layers. Diffraction from pure KCl and KI are observed, which indicates almost complete segregation.

coherence lengths ~ 500 Å perpendicular to the surface although the growth cross section was only ~ 50 Å parallel to the surface, owing to the columnar growth of the segregated salts. RbF and RbI segregation is also evident from the RHEED spectra shown in Fig. 10(a). No x-ray diffraction peak for pure RbF was visible, probably because our x-ray diffraction study was performed in the air and RbF is very hygroscopic. Atmospheric moisture causes a RbF film to deteriorate immediately when it is removed from the vacuum. Similar segregation was also observed for NaF+NaI, KF+KI, and NaCl+RbCl, when codeposited.

By using low substrate temperatures $T_g \approx -100$°C, however, we have also been able to grow single-crystal metastable-disordered alkali halide alloys KCl_xI_{1-x} with $x \approx 0.5$, which do not exist on the bulk phase diagram. They are stabilized epitaxially, presumably by forced atomic registry with the substrate, in a manner, predicted earlier,[19] entirely analogous to that for semiconductor systems such as $GaAs_xSb_{1-x}$.[20] A (002) x-ray Bragg scan of $KCl_{0.5}I_{0.5}$ and rocking curve on a KBr film grown on NaCl are shown in Fig. 9(b). The RHEED pattern for this alloy surface is shown in Fig. 10(b). Use of thin film substrates for this purpose is essential, because the alloy Bragg peak would otherwise be overwhelmed by the substrate reflection, as shown in Fig. 5. New ordered compounds, such as $NaRbCl_2$, that are also predicted to form by epitaxial stabilization have not yet been observed in our experiments, despite protracted efforts to detect them.

D. Superlattices

We have successfully grown superlattices of good quality using pairs of miscible alkali halides, even with $\sim 5\%$ lattice mismatch between the two salts. Figure 11(a) shows the x-ray diffraction spectrum of a KCl/RbCl superlattice with 50 periods and a wavelength of ~ 50 Å, grown at $T_g = -50$°C. NaCl was used as the substrate with ~ 500 Å of KCl buffer layer grown before the superlattice. The figure shows the fundamental peak of the superlattice located at $2\theta \approx 27.6$°, shifted ~ 0.6° from the much weaker diffraction peak of the KCl buffer layer. The two first-order satellites are visible on either side of the fundamental diffraction, separated from it about 2°. The coherence length and mosaic spread are estimated from the central diffraction peak to be ~ 1000 Å and ~ 0.5°, respectively. The RHEED spectrum shown in Fig. 10(c) remained virtually unchanged throughout the growth. It has not yet been possible to establish whether or not KCl and RbCl form coherent interfaces. The interface structure, including possible interdiffusion are the subject of ongoing investigations.

All efforts to grow superlattices of immiscible alkali halides failed. Several systems including KCl/KI, NaCl/RbCl, and RbF/RbI were studied. It is interesting to notice for the KCl/KI system that when successive monolayers of each pure salt were deposited alternately on a KBr substrate, a single-crystal disordered alloy of rather poor quality was formed. When the wavelength was increased, segregated growth of oriented columns of each pure salt were observed. X-ray diffraction from 1:1 and 5:5 KCl/KI superlattices grown in this way 1400 and 3400 Å thick, respectively, as are shown in Figs. 11(b) and 11(c). Only a broad alloy peak without satellites is seen for (1:1) KCl/KI superlattice, whereas the 5:5 superlattice shows two strong peaks. These correspond to diffraction from pure KCl and KI. They fall on either side of the weak KBr buffer layer peak. For the NaCl/RbCl and RbF/RbI system, in contrast, the segregation of the pure salts into columnar growth took place regardless of the wavelength and temperature.

IV. DISCUSSION

In this section we interpret the observed alkali halide growth in the context of the current understanding of alkali halide properties as reviewed in the Introduction. The behavor is also compared with that of metals and semiconductors in order to broaden the available perspective on the way MBE growth characteristics change from one crystal type to another.

The most important fact revealed by the present work is that alkali halides can be grown epitaxially at rates of tens of monolayers per second at temperatures down to ~ 100 K. We interpret this as an experimental demonstration that the activation energy E_s for surface diffusion of the ionic molecule is ≤ 0.2 eV. The RHEED data indicate that the (100) terraces during growth may be $\sim 10^2$ lattice planes in length, or $L \geq 10^2$ Å. If all the incident flux is incorporated into the ledges by diffusion in ≤ 0.1 sec, the surface diffusion coefficient at 100 K must be $D_s \geq L^2/0.1 \geq 10^{-11}$ cm^2/sec. A prefactor $D_0 \sim 10^{-3}$ cm^2/sec is expected as a simple combination of atomic frequencies ($\sim 10^{12}$/sec) and distances ($\sim 3 \times 10^{-8}$ cm). This identifies an activation energy $E_s \leq 0.2$ eV, for $kT_g \sim 0.01$ eV or $T_g \sim 100$ K.

Three points are worth mention in connection with this deduction. First, of course, the present results provide only an upper estimate of E_s because it was not possible to cool the substrate below 120 K to freeze out the growth. Second, in ongoing investigation of MgO, which melts at ~ 3000 K, we find that good growth persists at ~ 150 K. The pattern of behavior thus appears to be reproduced in highly ionic rocksalt oxides also. A paper currently in preparation describes the oxide growth more fully. Finally, it is important to note that the experimental findings are in good quantitative accord with theoretical expectations. Specifically, the theory predicts generally weak coupling of charged ions and molecules to the (100) terraces of the rocksalt structure.[14] Explicit estimates[12,14] for ions on KCl give activation energies for motion ~ 0.23 eV. These results follow from the general charge structure, and are thus expected to have an approximate general validity for all strongly ionic materials. This is undoubtedly the origin of the low growth temperatures established in the present research.

Heteroepitaxy of a second alkali halide on a foreign alkali halide surface has been found to be more complex but retains many of the same features. Two critical steps may be identified. First is the nucleation of incident molecules into crystals growing on a foreign surface. Second is the generally rapid relaxation of strain, which transforms the surface into the characteristic geometry of the pure alkali halide made from the foreign molecules alone. Thereafter the heteroepitaxial growth becomes identical with homoepitaxy of the foreign molecules. The following comments pertain to the nucleation process and to the subsequent strain relaxation.

In connection with the initial nucleation of a foreign film it is worth noting that the interionic spacing in the ionic molecules is much less than that of corresponding solid [the difference is in the range of 16–21 % (Ref. 20)]. Modest effects on the surface mobility can be expected from this cause. The most striking changes, however, occur when the foreign molecules reach the ledges for incorporation into the crystal. This can be accomplished only if the molecule is stretched to match the host lattice. Two alternatives are (1) that the surface fields automatically provide this stretching and that the smaller molecules are incorporated without delay, or (2) that the incorporation requires thermal activation. Our observations seem to indicate that both alternatives play a role in the incorporation process. Which predominates depends on temperature and the lattice misfit. Fast homoepitaxial growth at low temperatures, and the general tendency towards better growth for large molecules on small lattices than for small molecules on large lattices suggest that surface fields dominate the incorporation process in some cases. However, other observations also point to the need for thermal activation in the incorporation process. One is that unusually small molecules such as fluorides cannot be grown on foreign substrates as good single crystals. We interpret this as evidence that thermal activation requires temperature above $\sim 0.6T_m$ where the surface is, in any event, evaporating too rapidly for crystal growth. Similarly, KBr grown on NaCl at 0 °C, and RbCl grown on NaCl at -60 °C both have poor surfaces with very broad RHEED streaks near the beginning of growth. Similar problems are less apparent at higher growth temperatures or when the misfit is small. It seems likely that these phenomena have their origins in the activation process required to incorporate molecules into the (100) ledge structure.

There has been much work on semiconductors and some for metals in which the relief of stresses in pseudomorphic films has been investigated.[21,22] If a good strained film can indeed be obtained at low coverage, there is a general tendency for dislocations nucleated during subsequent growth to move to the interface and relieve the strain. The details of this process are not well understood. However, for a lattice mismatch δ the elastic energy of the film varies as $\delta^2 t$, with t the thickness, whereas the dislocation density (and hence energy) needed to completely relieve the strain is proportional to δ and independent of t. Strain relief is thus expected at a critical thickness t_c that depends linearly on dislocation energy and inversely on misfit δ. For modest misfits $\sim 1\%$, t_c is typically $> 10^3$ Å for semiconductors[21] and $> 10^2$ Å for metals.[22] More important, the experiments show that metallic films relax easily to their natural lattice spacing at the growth temperature, whereas the less mobile dislocation structure in semiconductors generally inhibit complete relaxation.

From the film thickness at which relaxation takes place it is possible to estimate the total strain energy prior to relaxation. This gives an upper bound on the energy of the eventual relaxed interface. The pseudomorphic strains are so large for alkali halides that linear elastic theory is not adequate. For this reason we have adapted the Harwell *PLUTO* program[23] to predict the strain energy. Figure 12 gives the interfacial energy per molecule, E_i, estimated from the misfit strain energy, E_m, and the observed critical film thickness, t_c, where $E_i \sim E_m t_c$.[24] For small misfits the energy seems to depend linearly on

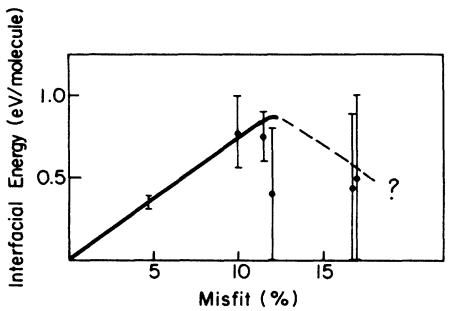

FIG. 12. Estimated interfacial energies, E_i, for various lattice misfits of alkali halides. The upper bound of the data for lattice misfits larger than 11% are the bulk strain energies for one monolayer, because the relaxation was observed to take place within the first monolayer.

the misfit as expected for dislocation models which relieve the strain energy using a density of interfacial dislocations proportional to the misfit. With about 1 eV per molecule for 10% misfit this corresponds quite reasonably to ~ 10 eV per molecule of dislocation length. It is notable in Fig. 12 that for large misfits $\geq 11\%$ the energy seems to saturate or decrease. In these cases the film relaxes in a single layer and the upper limit of the energy follows from the strain energy of a single complete layer.

To avoid the errors introduced by elasticity approximations in the case of large lattice misfit, we evaluated the bulk misfit strain energy density, E_m, for alkali halide thin films with in-plane strains as $E_m(\varepsilon)=E(\varepsilon)-E_0$, where $E(\varepsilon)$ and E_0 are the cohesive energy densities of strained and unstrained crystals, respectively. The Harwell PLUTO program, which is based on the well-established shell model,[25] was used to calculate the values of $E(\varepsilon)$ and E_0 numerically. Shell-model parameters for the various alkali halides were taken from the Harwell handbook.[23] Since there can be no stress perpendicular to the strained film, the film was allowed to relax completely normal to the plane in our calculations. The minimum relaxed energy was used to obtain the actual misfit strain energy, E_m, for Fig. 12.

It is possible to fit all these observations to the facts of alkali halide structure in a qualitative but fairly satisfactory way. We visualize that the relaxed interfaces consist of (100) terraces laid against each other almost fully relaxed, with very little distortion of their incommensurate lattices. This explains why the surface of the substrate and epilayer are found to be accurately parallel. Furthermore, it appears likely that the (100) ledges on the two interfaces must orient parallel to each other so that large regions of misfit between the two surfaces are avoided. Thus, the accurate in-plane alignment of the cubic axis may arise from a sort of atomic scale graphoepitaxy related to the prominent ledge structure (Fig. 1). Finally, the energy associated with the relaxed interfaces points to a dislocation description of the strain accommodation where the misfit is relatively small. For large misfit, however, the extensive relaxation that arises from weak bonding across the (100) cleavage planes probably makes dislocation concepts largely irrelevant to the discussion of the resulting structure. Rather, to zeroth order, the two surfaces should probably be regarded as undisturbed. The interface thus contains all relative phases of the two surfaces, regardless of the precise misfit. The energy then becomes independent of δ, as observed (Fig. 12) when the misfit is larger than 10%. The residual elastic interactions are expected to be weaker for larger lattice spacings and for heavier atoms which are more polarizable.

Information about the kinetics of molecular incorporation into the ledges is available from efforts to create alkali halide alloys described above. Two distinct phenomena are involved. First, ledge misfit apparently causes the incorporation at various ledges to be biased in favor of one species or the other. Thus, in the observed columnar growth, the alternating columns are spaced by distances comparable with the ledge separation. It is easy to understand how a given ledge can operate preferentially when its environment is saturated with one particular species of the two. Nevertheless, in its progress across a growing surface, any given ledge must pass from one column to the next, which contain the opposite species, whereupon the ledge action must change to accommodate this second species. At present these mechanisms are not at all understood. A single success in growing the metastable alloy occurred for KCl_xI_{1-x} with $x\sim 0.5$, in which the mismatch is about 12%. Apparently this is not sufficient for the selection mechanism to operate. It is equally interesting that metastable ordered compounds such as $NaRbCl_2$, for example, are predicted to form epitaxially under the influence of a foreign epitaxial constraint, but in no case was any observed. In both cases, continuous growth of an alloy requires an appropriate surface template, and it may be that the failure begins with the first monolayer of coverage. Regardless of these factors the incorporation energy ~ 1.5 eV at the ledges is much too large for local equilibrium to be achieved

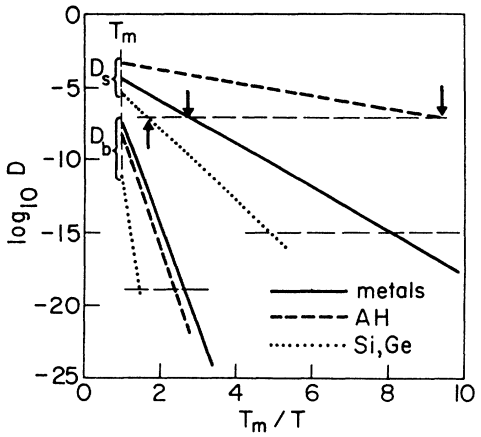

FIG. 13. Diagram showing deduced global dependences of surface and bulk diffusion coefficients, D_s and D_b, on T_m/T for metals (solid lines), elemental semiconductors (dotted lines), and strongly ionic salts (dashed lines). The construction is described in the text. Smooth flat interfaces generally require $D_s \geq 10^{-8}-10^{-7}$ cm^2/sec, which fixes the lowest growth temperatures (arrows) as $\sim 3T_m/8, 0.55T_m$, and $0.1T_m$ in the three cases. RHEED oscillation are expected for $D_s \geq 10^{-15}$ cm^2/sec.

among alternative species at low temperatures, as this requires detailed balance. Consequently, ordered ternary compounds would not be expected to form even if they were thermally stable. All these alloying phenomena thus reflect the kinetics of incorporation, but in a way that is not fully understood at present.

The results presented above make it possible, for the first time, to compare the MBE growth characteristics of strongly ionic solids with those of metals and semiconductors. For this purpose a figure giving typical bulk and surface diffusion coefficients D_b and D_s as function of temperature is most useful.[5] For metals there is only a small temperature range near $T_g = 3T_m/8$ at which $D_s > 10^{-7}$ cm^2/sec, in order to achieve smooth growth, while $D_b < 10^{-19}$ cm^2/sec in order to avoid monolayer interdiffusion at interface. This problem is absent for semiconductors, but the generally more sluggish diffusion requires growth temperatures $\geq 0.55T_m$. For alkali halides the situation established in this research is quite different. Surface diffusion is so fast that growth proceeds rapidly even at $T_g \sim 0.1T_m$. The surface diffusion rate consistent with those observations and $D_0 \sim 10^{-3}$ cm^2/sec is shown in Fig. 13 for comparison with the cases of metals and semiconductors. That D_s is so much larger for salts is a consequence of the weakly corrugated surface potential, as described above. In other work we have found very similar results for the growth of MgO, which is a relatively ionic oxide. From the present work, however, the characteristic MBE conditions for ionic salts appear well defined and qualitatively distinct from those of other materials types. It will be of interest in the future to compare these results with those for systems of intermediate ionicity, such as transition-metal oxides or II-VI compounds, for example.

ACKNOWLEDGMENTS

We thank M.V. Klein for generously providing single-crystal substrates. This research was supported in part by the U.S. Department of Energy under Contract No. DE-AC02-76ER01198.

[1] *Molecular Beam Epitaxy,* edited by C. T. Foxon and J. J. Harris (North-Holland, Amsterdam, 1987).

[2] *Heteroepitaxy on Silicon,* edited by J. C. Fan and J. M. Poate (Materials Research Society, Pittsburgh, PA, 1986).

[3] *Metallic Multilayers and Epitaxy,* edited by M. Hong *et al.* (The Metallurgical Society, Warrendale, PA, 1988).

[4] J. E. Cunningham, J. A. Dura, and C. P. Flynn, in *Metallic Multilayers and Epitaxy,* Ref. 3, p. 77.

[5] C. P. Flynn, J. Phys. F **18**, L195 (1988).

[6] Lower limits of growth are approximately as follows: for Si, 900 K ($\sim 0.54T_m$, see, e.g., H. P. Zeindl *et al.*, in Molecular Beam Epitaxy, Ref. 1) and for Ge, 600 K [$\sim 0.5T_m$, see, e.g., P. W. Sullivan, Appl. Phys. Lett. **44**, 190 (1984)].

[7] M. P. Tosi, in Vol. 16 of *Solid State Physics,* edited by F. Seitz and D. Turnbull (Academic, New York, 1964), p. 1.

[8] R. P. Lowndes and D. H. Martin, Proc. R. Soc., Ser. A **308**, 473 (1969).

[9] R. S. Roth, M. A. Clevinger, and D. McKenna, *Phase Diagrams for Ceramists* (American Ceramic Society, Columbus, Ohio, 1984).

[10] C. P. Flynn, *Point Defects and Diffusion* (Oxford University Press, Oxford, 1972).

[11] B. J. Stein and H. J. Meyer, J. Cryst. Growth **49**, 696 (1980).

[12] R. B. Bjorklund and K. G. Spears, J. Chem. Phys. **66**, 3448 (1977); **66**, 3437 (1977).

[13] W. Lasser, H. Dabringhaus, and H. J. Meyer, J. Cryst. Growth **62**, 248 (1983).

[14] J. E. Hove, Phys. Rev. **99**, 430 (1955).

[15] M. H. Yang and C. P. Flynn, Phys. Rev. Lett. **62**, 2476 (1989).

[16] P. Williams and G. Gillen, Surf. Sci. **180**, L109 (1987).

[17] For example, L. Friedman, J. Chem. Phys. **23**, 477 (1955).

[18] Calculated according to Eq. (3.13), $t = 0.9\lambda/[B\cos(\theta_B)]$, where B is the full width at half maximum of the reflection, from B. D. Cullity, *Elements of X-Ray Diffraction* (Addison-Wesley, Reading, Massachusetts, 1978).

[19] C. P. Flynn, Phys. Rev. Lett. **57**, 599 (1986).

[20] *American Institute of Physics Handbook,* 3rd ed. (McGraw-Hill, New York, 1972).

[21] B. W. Dodson and J. Y. Tsao, Appl. Phys. Lett. **51**, 1325 (1987).

[22] Y. Kuk, L. C. Feldman, and P. J. Silverman, Phys. Rev. Lett. **50**, 511 (1983).

[23] Kindly supplied by Dr. J. Hardy of Harwell, *PLUTO* codes, and *Handbook of Interatomic Potentials* (UKAEA Harwell, 1981)

[24] J. W. Matthews, J. Vac. Sci. Technol. **12**, 126 (1975); see also, articles in *Epitaxial Growth,* edited by J. W. Matthews (Academic, New York, 1975), Parts A and B.

[25] V. V. Mitskevich, Fiz. Tverd. Tela (Leningrad) **5**, 3500 (1963) [Sov. Phys.–Solid State **5**, 2568 (1964)].

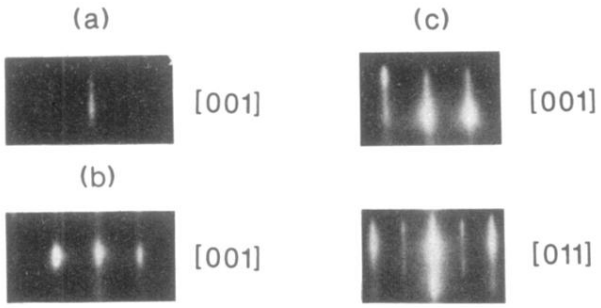

FIG. 10. RHEED patterns of (a) $RbF_{0.5}I_{0.5}$ approximately ten monolayers thick grown on RbCl, (b) KCl_xI_{1-x} with $x \sim 0.5$ grown on KBr, and (c) (KCl/RbCl) superlattice with 50 periods and a wavelength of ~ 50 Å, grown at -50 °C. The segregation of $RbF_{0.5}I_{0.5}$ into pure salts of RbF and RbI are shown clearly by the two sets of streaks in (a).

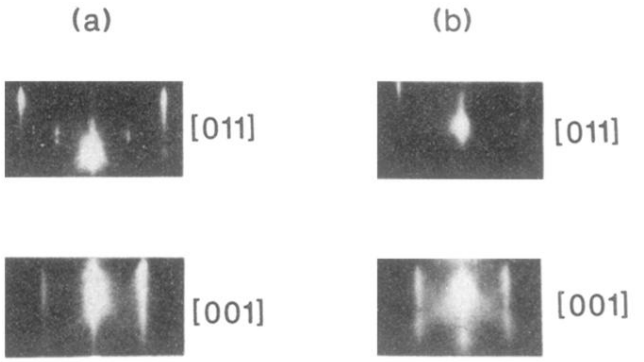

FIG. 3. RHEED patterns of (a) cleaved and evaporated NaCl after 200-Å regrowth at room temperature and (b) KBr(100) after 2 μm regrowth at $-145\,^{\circ}$C. See text for details.

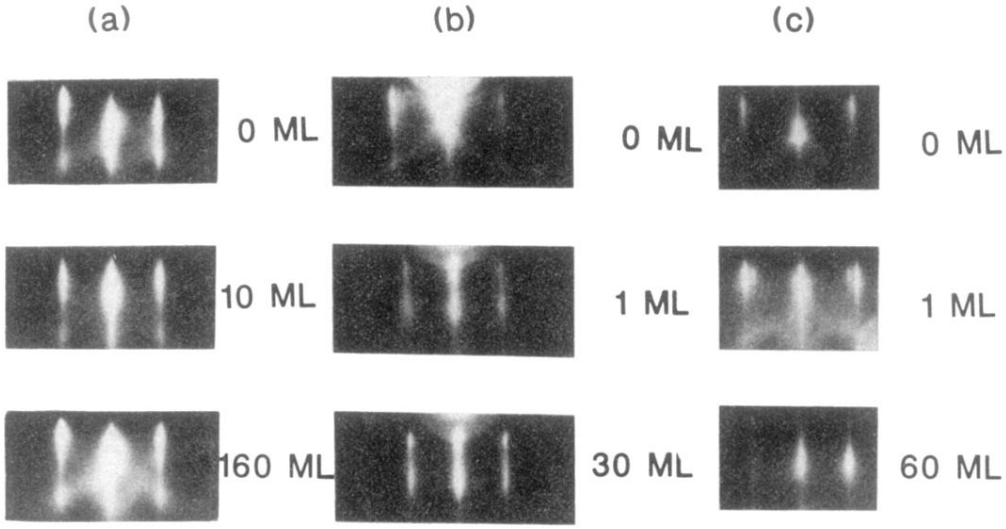

FIG. 6. Comparison of RHEED patterns of (a) KCl with different thicknesses grown on a RbCl substrate, (b) KBr grown on NaCl at 0 °C, and (c) RbCl grown on NaCl at 200 °C.

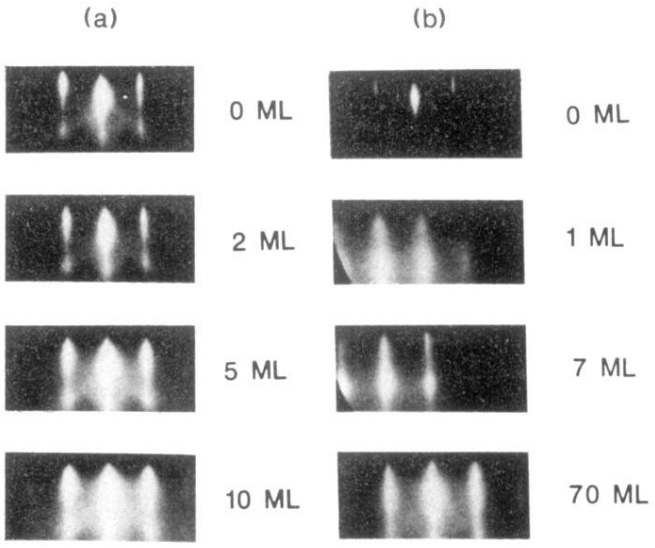

FIG. 7. RHEED patterns of NaCl with different thicknesses grown on KCl at (a) 200 °C and (b) −60 °C.

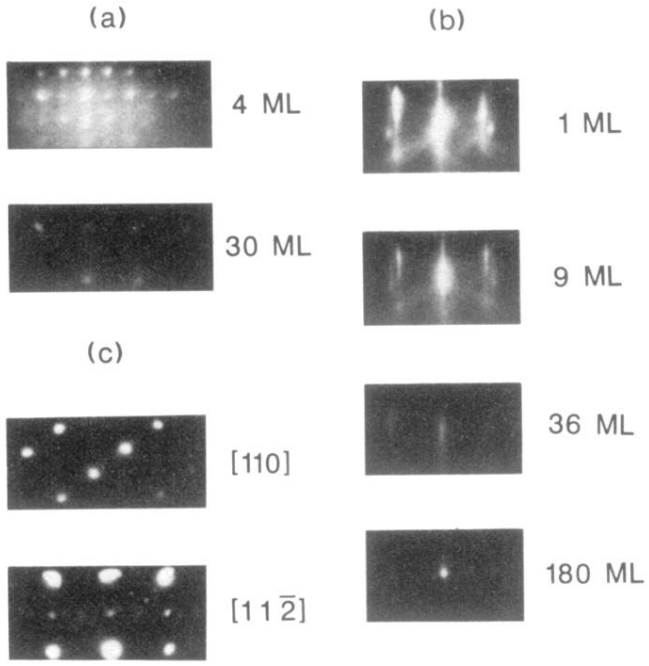

FIG. 8. RHEED patterns of (a) KF grown on NaCl, (b) KF grown on KCl, (c) KBr (111) grown on α-Al_2O_3(0001).